

https://dspace.org/

Assessing the geological relationships between the maficultramafic intrusion in the Haib area and the Vuurdood Subsuite Richtersveld Subprovince

Bibi Jogee; Grant Bybee; Laurence Robb; D.L Reid; H Minnaar ...

https://hdl.handle.net/10539/41133
WOS

Downloaded from a DSpace repository. https://dspace.org/

Assessing the geological relationships between the mafic-ultramafic intrusion in the Haib area and the Vuurdood Subsuite, Richtersveld Subprovince

B.A. Jogee and G.M. Bybee
School of Geosciences, University of the Witwatersrand, Johannesburg, South Africa
e-mail: bibi.jogee1@wits.ac.za; grant.bybee@wits.ac.za

L.J. Robb
School of Geosciences, University of the Witwatersrand, Johannesburg, South Africa
Department of Earth Sciences, University of Oxford, United Kingdom
e-mail: laurence.robb@earth.ox.ac.uk

D.L. Reid
Department of Geological Sciences, University of Cape Town, Cape Town, South Africa
e-mail: david.reid@uct.ac.za

H. Minnaar
Department of Geology, University of Free State, Free State, South Africa
e-mail: MinnaarH@ufs.ac.za

L. Caricchi
Department of Earth Sciences, University of Geneva, Switzerland
e-mail: luca.caricchi@unige.ch

R. Bolhar
School of Geosciences, University of the Witwatersrand, Johannesburg, South Africa
e-mail: robert.bolhar@wits.ac.za

© 2024 Geological Society of South Africa. All rights reserved.

Abstract

The Haib porphyry copper deposit is situated in the Richtersveld Subprovince and is host to unique Palaeoproterozoic porphyry copper mineralisation in Namibia. Several lines of evidence, including machine-learning geothermobarometry, indicate that the deposit is exposed at mid- to upper-crustal levels, as constrained from average pressure and temperature estimates of 4 kbar and 870°C, respectively. The Haib porphyry copper deposit is associated with, and is in close proximity to, a mafic-ultramafic intrusion named the Kokerboom Intrusion (KI) in this study. Together with several other mafic intrusions in this region, these intrusions are known collectively as the Vuurdood Subsuite of the Richtersveld Subprovince. The purpose of this study is to demonstrate a genetic link between the KI and the Vuurdood Subsuite using lithological characteristics, mineral and alteration assemblages, major and trace element geochemistry and U-Pb geochronology. Pyroxenites from the KI contain magmatic sulphides and have a geochemical affinity with shallow plutonic and volcanic rocks of the Haib porphyry, providing a unique mid-crustal perspective on porphyry copper deposit metallogenesis.

Downloaded from http://pubs.geoscienceworld.org/gssa/sajg/article-pdf/127/1/55/6373101/55_0011_jogee_et_al.pdf
by University of the Witwatersrand user

Introduction

Palaeoproterozoic igneous rocks form a large magmatic arc complex known as the Richtersveld Magmatic Arc (RMA), which is well exposed in the lower Orange River region of South Africa and Namibia (Macey et al., 2017). Recent studies have provided evidence for its formation during the period between 1 910 and 1 865 Ma, with subsequent incorporation into a Mesoproterozoic continental assembly, now preserved in the Namaqua-Natal tectonic province (Macey et al., 2017 and references therein). The RMA consists of a volcanic succession (the Orange River Group) intruded by a mainly granitic batholith (the Vioolsdrif Suite), with compositions ranging from ultramafic to felsic (Figure 1). The ultramafic end member of the Vioolsdrif Intrusive Suite (VIS) is known as the Vuurdood Subsuite. Epiclastic sedimentary lithologies occur locally, interpreted as reworked lavas and welded tuffs and products of erosion and re-deposition of exhumed granitic members of the batholith, and also as extraneous transported material tectonically juxtaposed during Meso- and Neoproterozoic orogenesis (Macey et al., 2017). The VIS of the RMA hosts the Haib porphyry copper deposit (Figure 2). This deposit is unique as it may be the only known occurrence of this specific style of mineralisation in southern Africa and one of the few occurrences globally of Precambrian porphyry copper mineralisation (Meng et al., 2021).

The current study focuses on mafic-ultramafic intrusions that occur throughout the batholith, as numerous, relatively small intrusions (Figures 1 and 2). Many of them appear to have been emplaced before, and subsequently disrupted by, later granitic intrusions of the VIS (Reid and Minnaar, 2021). They have been assigned to a lithostratigraphic unit known as the Vuurdood Subsuite of the VIS. Much of our knowledge of these early mafic-ultra mafic components of the batholith has been confined to localities in the Vioolsdrif area of South Africa, but several intrusions have now been identified in the vicinity of the Haib copper deposit in Namibia. This paper assesses the petrogenetic links (if any) between the mafic-ultramafic intrusions associated with mineralisation of the Haib deposit and the known intrusions of the Vuurdood Subsuite, using petrography, major and trace element geochemistry, as well as U-Pb ages determined for these units.

Geological setting

The Mesoproterozoic (~1.1 Ga) Namaqua-Natal Province (NMP) is a major orogenic belt that extends from Lüderitz on the west coast of Namibia to the eastern (KwaZulu-Natal) coast of South Africa. It comprises igneous and metamorphic rocks that formed or experienced metamorphism during the Namaqua Orogeny (Cornell et al., 2006; Macey et al., 2017; van Niekerk et al., 2022). The Namaqua "Sector" of the Namaqua-Natal Province consists of five tectono-stratigraphic terranes, namely (from west to east) the Richtersveld and Bushmanland subprovinces, and the Kakamas, Areachap and Kaaien domains (Cornell et al., 2006; Macey et al., 2017). The westernmost Richtersveld Subprovince is composed of the oldest (Palaeoproterozoic) supracrustal rocks in the NMP. It is tectonically bounded by the Bushmanland Subprovince and Kakamas Domain by thrusts or subvertical shear zones (Cornell et al., 2006; Macey et al., 2017). In the west, southeast-directed thrust and transpressive shear zones transported part of the

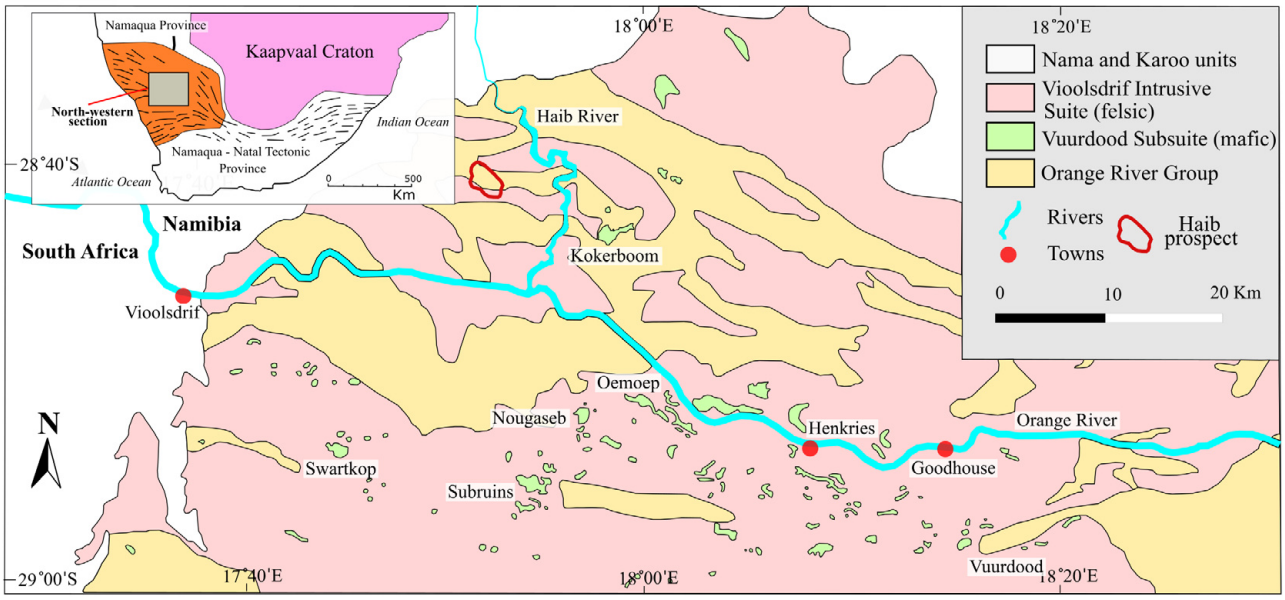


Figure 1. *Simplified geological map of the Richtersveld Magmatic Arc (RMA) in the Vioolsdrif-Haib area, showing the distribution of the Orange River Group (ORG), Vioolsdrif Intrusive Suite (VIS) and the main localities of the Vuurdood Subsuite (Minnaar and Reid, 2021). Inset shows the position of map with reference to the Namaqua-Natal tectonic province and the Kaapvaal Craton. The RMA is located in the north-western section of the Namaqua-Natal tectonic province. In this study, the Kokerboom Intrusion (KI) is comprehensively sampled and compared with literature data from the Vuurdood Subsuite in the Northern Cape Province of South Africa.*

Downloaded from http://pubs.geoscienceworld.org/gssa/sajg/article-pdf/127/1/55/6373101/55_0011_jogee_et_al.pdf
by University of the Witwatersrand user

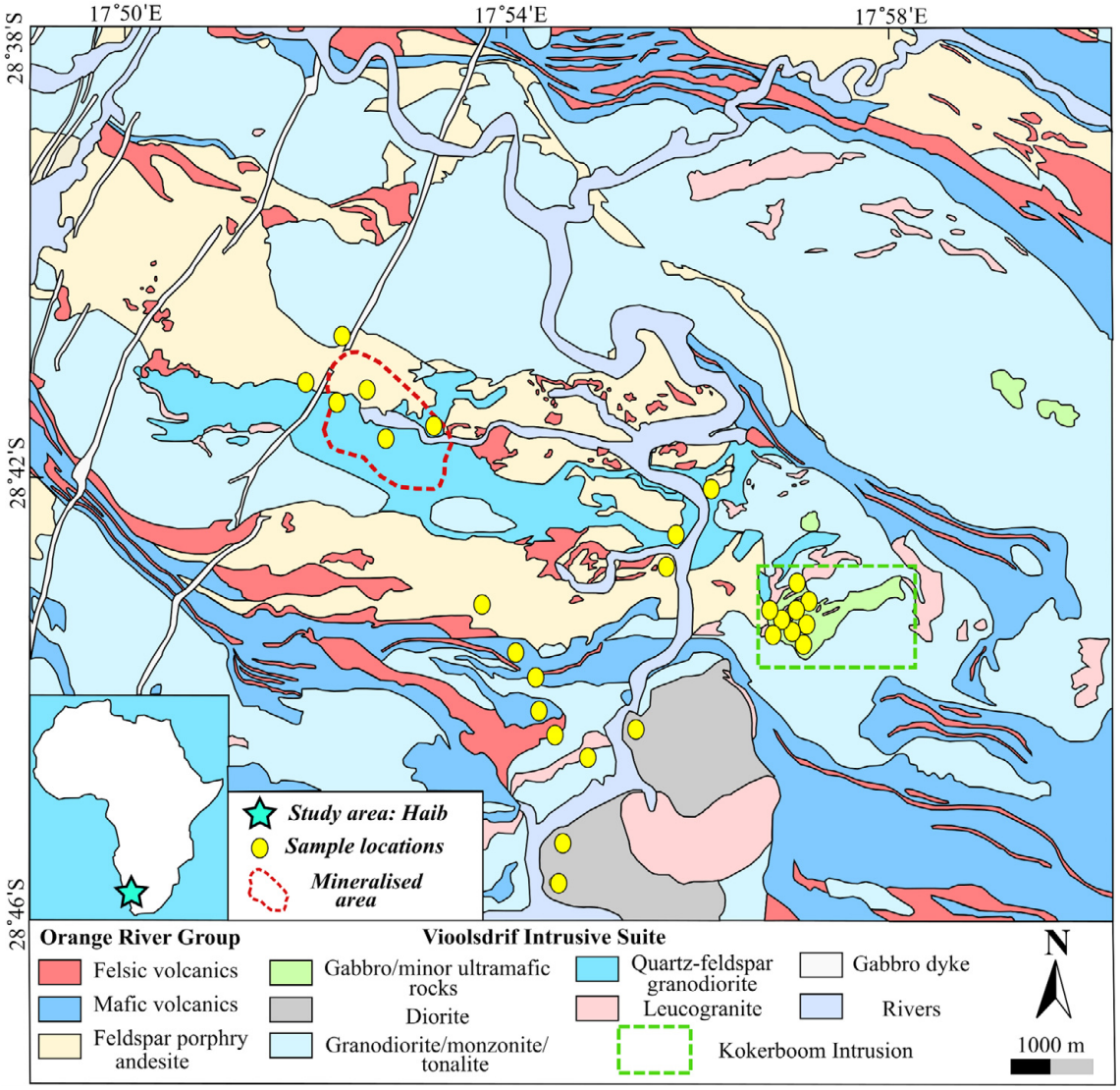


Figure 2. *Geological map of the Haib porphyry copper-molybdenum deposit with sample locations from this study. Map modified from Minnitt (1979) and Meng et al. (2021).*

Neoproterozoic Gariep Group over the Richtersveld Subprovince during the "Pan-African" orogeny (Cornell et al., 2006; Macey et al., 2017). The Richtersveld Subprovince covers an area of approximately 29 000 km² and forms an approximately 200 km-wide, wedge-shaped crustal block, composed of calc-alkaline volcanic and plutonic rocks (including the poorly-studied mafic-ultramafic intrusions of the Vuurdood Subsuite) that were formed in an island-arc setting (Reid et al., 1987; Reid, 1997; Cornell et al., 2006; Macey et al., 2017). According to Joubert (1986) and Macey et al. (2017), the Richtersveld Subprovince is composed of two zones of different tectono-metamorphic domains:

- a western section, known as the Vioolsdrif Domain, composed of Palaeoproterozoic rocks that underwent greenschist-facies metamorphism and were not pervasively reworked during the Namaqua Orogeny, and
- an eastern section, known as the Pella Domain, composed of Palaeoproterozoic rocks that were pervasively overprinted during the Namaqua Orogeny.

The Haib porphyry copper-molybdenum deposit is situated in the former and is host to disseminated, vein- and shear-zone-localised copper mineralisation (Minnitt, 1979; Minnitt, 1986; Barr and Reid, 1992; Colliston and Schoch, 2000; Walker and Richards, 2018; Vermond, 2019). The shear-zone-localised mineralisation is associated with early dark micaceous veins (EDM veins) (Meng et al., 2021). Argillic and propylitic alteration assemblages are missing, instead potassic and chlorite-sericite alteration is dominant (Minnitt, 1979; Minnitt, 1986; Vermond, 2019; Meng et al., 2021).

Lithostratigraphy

The Richtersveld Subprovince consists of an older volcano-sedimentary sequence, the Orange River Group (ORG), which was intruded by an extensive composite and cogenetic suite of plutonic rocks, the VIS (Minnitt 1979, 1986). The age range for the Richtersveld Subprovince is between approximately 1 910 to

Downloaded from http://pubs.geoscienceworld.org/gssa/sajg/article-pdf/127/1/55/6373101/55_0011_jogee_et_al.pdf
by University of the Witwatersrand user

1 865 Ma, based on U-Pb geochronology on zircon and rutile (Meng et al., 2021). The ORG is composed of subaerial volcanic rocks ranging in composition from basaltic andesite to rhyolite, and cogenetic pyroclastic rocks, including ignimbrite and welded lapilli tuff (Figure 2; Reid 1977; Reid, 1979a, 1979b, Minnitt, 1986; Reid et al., 1987; Cornell et al., 2006; Macey et al., 2017; Meng et al., 2021). The VIS is composed of mafic-ultramafic intrusions, diorite, tonalite, granodiorite, monzogranite, quartz-feldspar porphyry (QFP) granodiorite and leucogranite (Figure 2; Reid 1977; Reid, 1979a, 1979b, Minnitt, 1986; Reid et al., 1987; Cornell et al., 2006; Macey et al., 2017; Meng et al., 2021). The ORG has been subdivided into two subgroups, the De Hoop and the Haib subgroups, within which several formations are recognised (Reid, 1979a; Cornell et al., 2006; Minnaar, 2012; Macey at al., 2017). In the Haib area, the Haib Subgroup of the ORG has been further subdivided into the basal volcanic Tsams Formation and the overlying volcanic Nous Formation (Blignault, 1977; Minnitt, 1986).

Within this lithostratigraphic framework, the Haib porphyry copper deposit is hosted by the coeval and comagmatic ORG and VIS (Minnitt, 1979 and Minnitt, 1986). The volcanic rocks, belonging to the Tsams Formation of the ORG, are interlayered aphyric rhyolites, phyric rhyolites, plagioclase-phyric andesites and mafic tuffs. The plutonic rocks, represented by a composite plutonic mass belonging to the VIS, intrude the volcanic rocks of the Tsams Formation. The VIS is subdivided into several subunits, known as the Vuurdood Subsuite (mafic-ultramafic), Gaobis Diorite, Khoromus Porphyry, Goodhouse Subsuite (Granodiorite) and the Ramansdrif Alkali Granite (Minnitt, 1979, 1986). It is the poorly-described clinopyroxenites and gabbros of the Vuurdood Subsuite that form the subject of this work, which are named the Kokerboom Intrusion in this study.

The Vuurdood Subsuite

The mafic-ultramafic rocks of this subsuite are geologically important but volumetrically minor (Minnitt, 1979; Reid, 1987; Reid and Minnaar, 2021). These mafic-ultramafic intrusions are predominantly exposed in the Northern Cape province (South Africa), but extend into southern Namibia (Figure 1; Minnitt, 1979; Reid and Minnaar, 2021). The intrusions are recognised in the field by their distinct dark colour and resistance to erosion (Reid and Minnaar, 2021).

The Vuurdood Subsuite consists of lithologically composite intrusions, predominantly composed of meta-gabbroic rocks with minor (~25%) peridotites and pyroxenites. The intrusions vary in size and shape, ranging from about 100 m to about 2 km across (Minnaar, 2011; Reid and Minnaar, 2021). The rocks are metamorphosed to amphibolite grade. The peridotites have been serpentinised with variable amounts of secondary amphibole and chlorite present. The gabbros and pyroxenites have been altered to coarse-grained amphibolites, the primary magmatic pyroxene-plagioclase assemblage has been replaced by actinolite-hornblende, secondary plagioclase, epidote, chlorite and quartz (Reid, 1987; Minnaar, 2011; Reid and Minnaar, 2021). In the Haib area, apparently similar rocks are located east of the Haib copper prospect and constitute several distinct gabbroic intrusions (Figures 1 and 2). For the purposes of this study, and following the practice of naming discrete ultramafic intrusions of the Vuurdood Subsuite, the mafic-ultramafic units in the Haib area will be referred to as the Kokerboom Intrusion (KI). The main intrusion in the Haib area is predominantly composed of gabbros and is pervasively intruded by leucogranite dykes and veins.

There are no published age data for the Vuurdood Subsuite but other rocks from the Vioolsdrif Domain of the RMA have been dated. The previous radiometric ages for the Vioolsdrif Domain of the RMA have been presented by Reid (1987), Grumbley (2015), Macey et al. (2017) and Meng et al. (2021) (Table 1 of the Supplementary Material). (Supplementary data files are archived in the South African Journal of Geology repository (http://doi.org/10.25131/sajg.127.0011.sup-mat)). Meng et al. (2021) conducted ID-TIMS U-Pb geochronology on zircon and rutile from the intermediate-felsic rocks of the VIS; results show that the RMA formed between 1 881 to 1 886 Ma, taking the 2σ uncertainty into account (Meng et al., 2021). This paper presents the first U-Pb zircon age data for the ultramafic to mafic component of the VIS known as the Vuurdood Subsuite.

Methodology

Details of the analytical procedures, including whole rock XRF, ICPMS, mineral liberation and zircon LA-SF-ICPMS as well as geothermobarometry, are detailed in the supplementary material. Analytical data are reported in Tables 2 and 3 of the supplementary material.

The Kokerboom Intrusion (KI) in the Haib area

The rocks show a range of mineralogical types, including gabbro (95%) and clinopyroxenites (5%). Clinopyroxenites are coarse-grained (~4 mm), dark grey-green, massive, composed of clinopyroxene altered to fibrous-granular actinolite, and contain disseminated and massive sulphides (chalcopyrite) (Figure 3a). Gabbros are coarse-grained (3 mm), grey-coloured with a distinct speckled appearance, equigranular and consist of pyroxene and plagioclase (Figure 3b).

Several intrusions are located east of the Haib River (Figure 1 and 2). The largest is ~2 km in diameter, predominantly gabbroic in composition, with grain-size and modal variations on the outcrop scale (Figure 3b). The contacts with the surrounding granodiorite are sharp, sheared or show signs of assimilation (Figure 4a to c). The KI is composed of clinopyroxenites and gabbros. The intrusion is pervasively intruded by leucogranitic dykes as well as minor leucogranitic veins. Distinct mingling textures can be observed along the contacts between the surrounding granodiorite and the gabbroic intrusion (Figure 4c).

Alteration is pervasive throughout the mafic-ultramafic complex and thus classification is based on the preserved primary mineral phases as opposed to the altered mineral assemblages.

Downloaded from http://pubs.geoscienceworld.org/gssa/sajg/article-pdf/127/1/55/6373101/55_0011_jogee_et_al.pdf
by University of the Witwatersrand user



Figure 3. *The plutonic lithologies of the Vlooldrif Intrusive Suite (VIS) in the Haib area. (**a**) Coarse-grained clinopyroxenite hand samples. (**b**) Gabbros showing grain-size variations on the outcrop scale. Certain sections of the outcrop are darker depicting a coarser grain size. (**c**) Distinctly speckled and equigranular gabbros.*

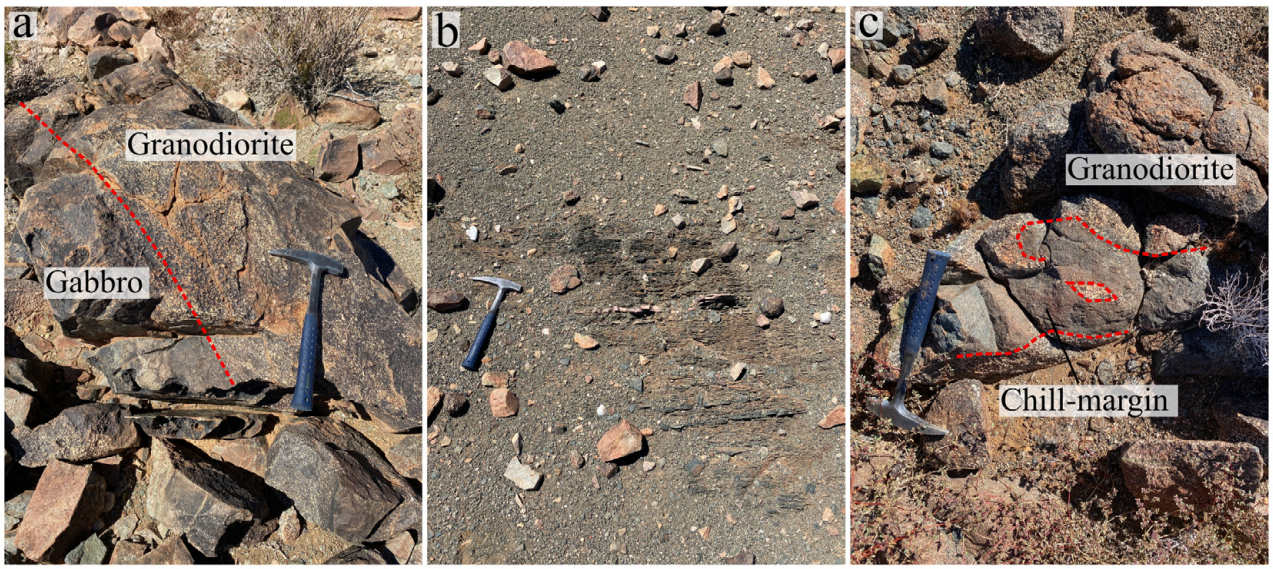


Figure 4. *The contacts of the main gabbroic body with the surrounding granodiorite. (**a**) A distinct sharp contact. (**b**) northwest-southeast-trending sheared contact. (**c**) Diffuse contact with mingling textures.*

Gabbro

The gabbro is medium- to coarse-grained (~3 mm), equigranular and composed of plagioclase (60%), clinopyroxene (20%), hornblende-actinolite (10%), quartz (7%), apatite (2%), rutile, sphene and magnetite (1%) (Figures 5a and 6a). Cumulus clinopyroxene is replaced by hornblende-actinolite-chlorite-epidote pseudomorphs. Primary stubby prisms of hornblende/actinolite are altered to chlorite and epidote, whereas plagioclase is pervasively altered to sericite and epidote and displays a myrmerkitic texture (Figure 5a). Intercumulus, primary hornblende contains inclusions of magnetite, rutile and quartz. Hornblende/actinolite exhibits exsolution lamellae or simple twinning. Quartz is anhedral and displays a distinct undulose extinction. Magnetite occurs as distinct bleb-like and disseminated grains.

Clinopyroxenite

The clinopyroxenite is coarse-grained (~4 mm), massive and composed predominantly of cumulus clinopyroxene (95%), altered to fibrous-granular actinolite with minor chlorite-epidote-hornblende (3%), rutile, sphene and sulphides (2%) (Figure 5c and 6c). Actinolite has a fibrolite texture and shows exsolution lamellae and simple twinning. Actinolite is altered to chlorite and epidote. Magnetite is disseminated throughout and is associated with rutile, sphene, chlorite and actinolite. Sulphides in the clinopyroxenite occur as coarse (~2 mm) bleb-like

Downloaded from http://pubs.geoscienceworld.org/gssa/sajg/article-pdf/127/1/55/6373101/55_0011_jogee_et_al.pdf
by University of the Witwatersrand user

aggregates of chalcopyrite rimmed by chalcocite-covellite assemblages, which are subsequently rimmed by haematite-magnetite-ilmenite assemblages (Figure 5c).

Below the new data for the mafic-ultramafic intrusion (in Namibia) will be supplemented and compared with literature data for Vuurdood Subsuite, which is the mafic component of VIS in South Africa.

Major and trace element geochemistry

The SiO_2, Al_2O_3, Fe_2O_3, CaO, TiO_2, Na_2O and K_2O versus Mg# diagrams show a general increase and a subsequent decrease in concentration from the primitive to more evolved lithologies of the mafic-ultramafic intrusion and Vuurdood Subsuite (Figure 7). The only exception occurs in peridotite and gabbro, where the Al_2O_3 contents decrease between Mg# 90 to 40 (Figure 7). For the mafic-ultramafic intrusion, the clinopyroxenite has the lowest concentrations of Al_2O_3, CaO, TiO_2, Na_2O and K_2O and the highest Mg#, whereas Al_2O_3, CaO, TiO_2, Na_2O and K_2O concentrations for the gabbro is higher, showing overall lower Mg# values. For the Vuurdood Subsuite from literature, the peridotite has the lowest TiO_2, Al_2O_3 and CaO concentrations and the highest Mg#, whereas the Al_2O_3 and CaO concentrations for the pyroxenite and gabbro from literature show a broad range (Figure 7). The AFM diagram illustrate a continuum of compositions from the mafic-ultramafic to felsic units of the RMA

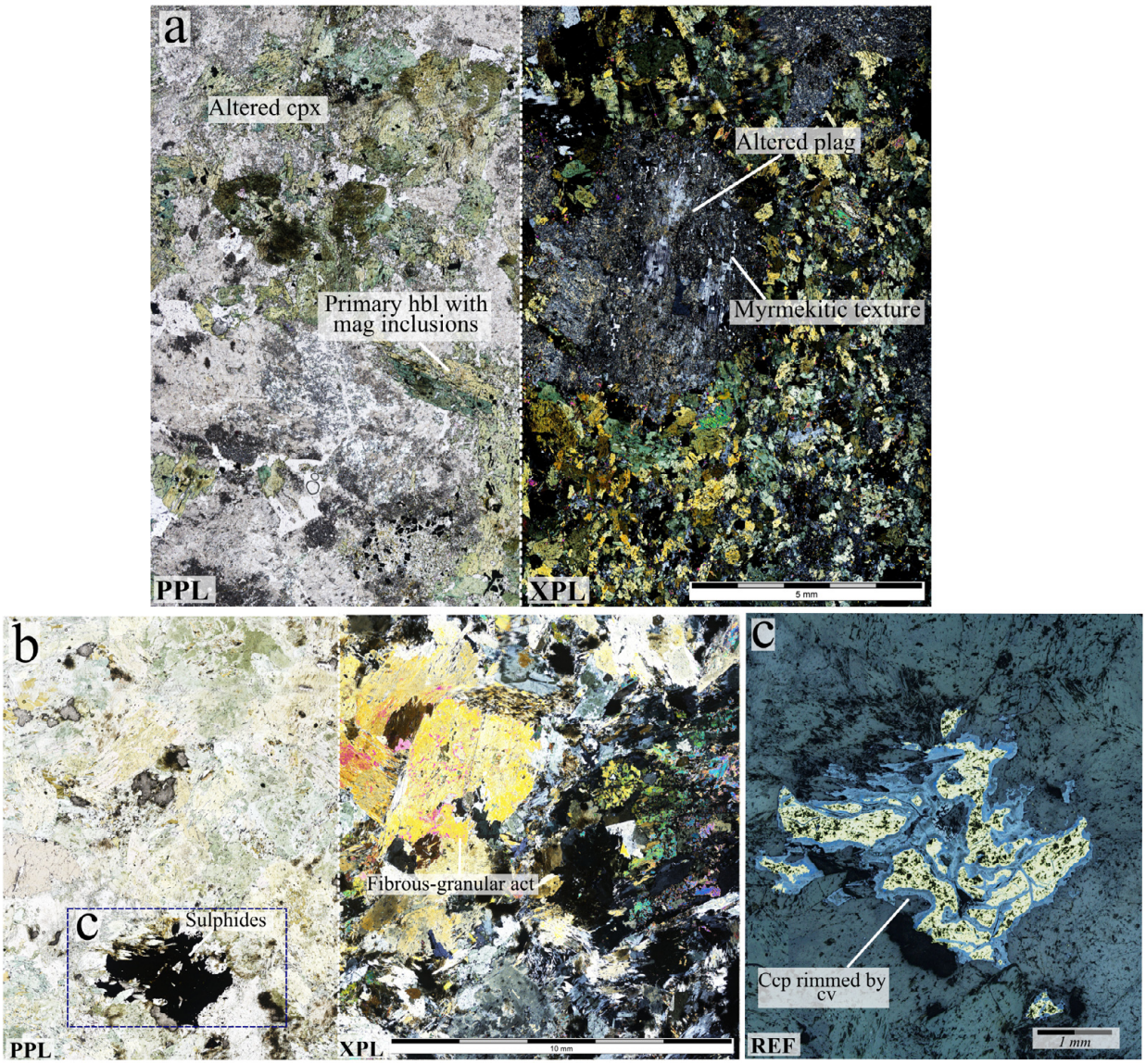


Figure 5. *Plane polarised light (PPL) and cross polarised light (XPL) photomicrographs of gabbro (a), and clinopyroxenite (b) of the mafic-ultramafic intrusion. (**a**) Primary stubby prisms of clinopyroxene are altered to hornblende (hbl), chlorite and epidote whereas plagioclase is pervasively altered to sericite and epidote and displays a myrmerkitic texture. (**b**) Sulphides in the clinopyroxenite. Fibrous-granular actinolite is evident. Primary clinopyroxene is altered to actinolite with minor chlorite and epidote and has inclusions of magnetite (mag). Opaque material is prevalent in the reflected (REF) light image. (**c**) Chalcopyrite (ccp) is being replaced by covellite (cv) and are rimmed by haematite-magnetite-ilmenite assemblages.*

Downloaded from http://pubs.geoscienceworld.org/gssa/sajg/article-pdf/127/1/55/6373101/55_0011_jogee_et_al.pdf
by University of the Witwatersrand user

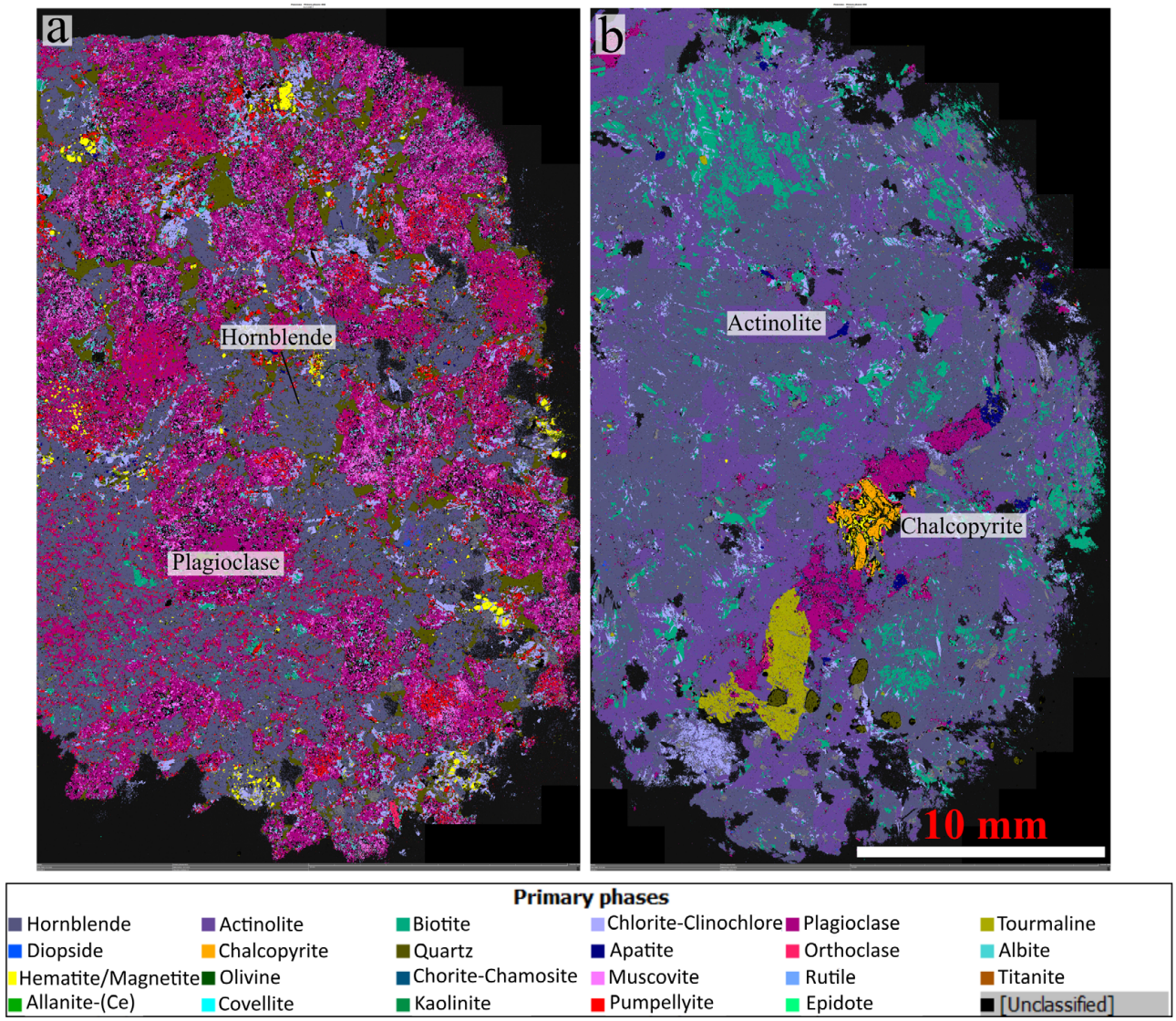


Figure 6. *False-colour maps produced using the Tescan Automated Mineral Analyser (TIMA) of representative thin sections for the gabbros (**a**), and clinopyroxenites (**b**). Modal abundances of plagioclase decrease from the gabbros to clinopyroxenites. From the mineral liberation maps the non-cotectic proportions of dominant mineral phases are clear.*

(Figure 8). The felsic plutonic units of the RMA plot in the calc-alkaline trend of the diagram whereas, the mafic units plot in both the calc-alkaline and tholeiitic trends of the diagram (Figure 8a and b). The quartz-feldspar-porphyry granodiorites of the Khoromus porphyry of the VIS are the host rocks of the Haib deposit. The section of the AFM diagram illustrating the various rock types constituting the mafic-ultramafic intrusion (Figure 8b) shows that the clinopyroxenite from the mafic-ultramafic intrusion plots in the tholeiitic trend , whereas the gabbro plots in both the calc-alkaline and tholeiitic trends (Figure 8). The AFM diagram also illustrates the various rock types constituting the Vuurdood Subsuite for comparison (Figure 8b) and shows that the peridotite and pyroxenite from literature plot distinctly in the tholeiitic trend, whereas the gabbro from literature plots in both the calc-alkaline and tholeiitic trends (Figure 8). In addition, the AFM diagrams shows that the mafic-ultramafic intrusion and the Vuurdood Subsuite overlap with average compositions of deep crustal cumulates from continental and island arc environments (Chin et al., 2018). The more evolved composition of the mafic-ultramafic intrusion and Vuurdood Subsuite trend towards the calc-alkaline array of the felsic and intermediate components of the VIS.

Chondrite-normalised REE patterns for the various rock types constituting the mafic-ultramafic intrusion are relatively flat, with lower abundances for the clinopyroxenite. The gabbro has slightly elevated concentrations and minor negative Eu anomalies (Figure 9a). Mid-oceanic ridge basalt (MORB)-normalised, multi-element variation patterns for the various rocks of the mafic-ultramafic intrusion show a distinct decoupling between the large ion lithophile elements (LILE) and high field strength elements (HFSE) (Figure 9b). The LILE are elevated relative to the HFSE. A distinct variation is observed

Downloaded from http://pubs.geoscienceworld.org/gssa/sajg/article-pdf/127/1/55/6373101/55_0011_jogee_et_al.pdf
by University of the Witwatersrand user

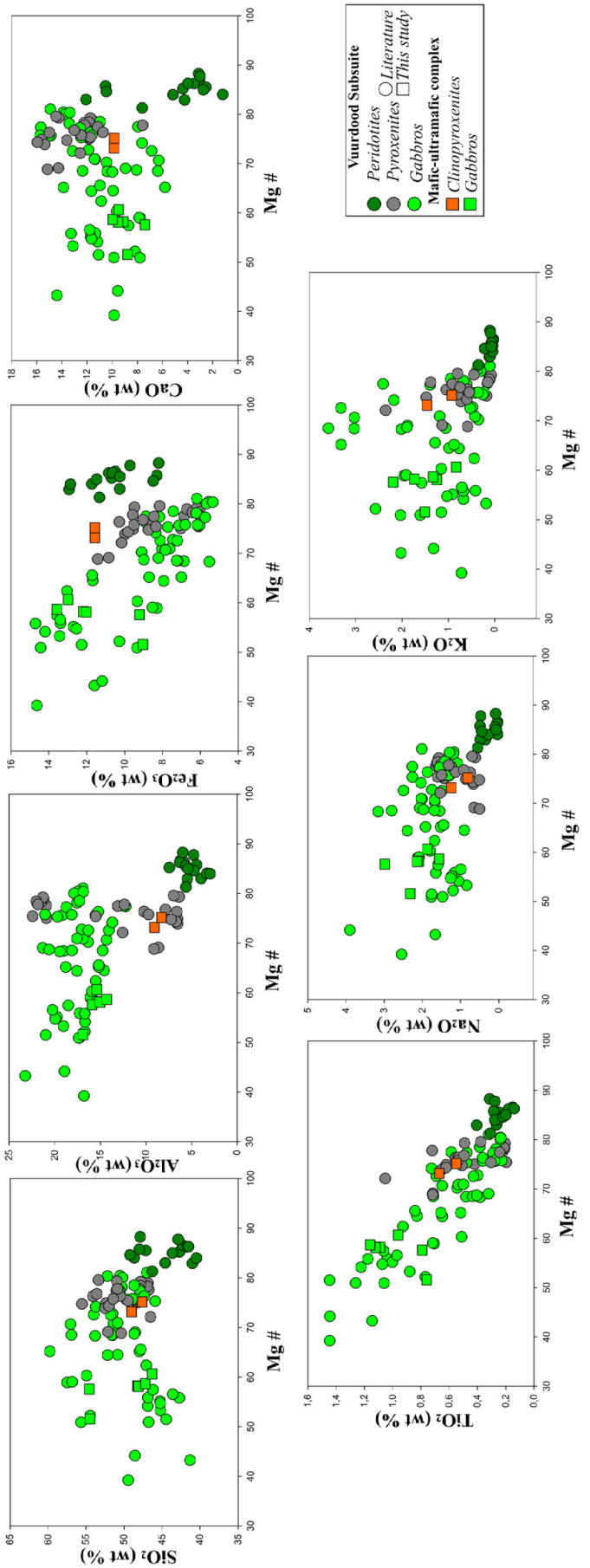


Figure 7. *Diagrams showing SiO_2, Al_2O_3, Fe_2O_3, CaO, TiO_2, Na_2O and K_2O versus $Mg^{\#}$. Oxide compositions decrease from the primitive to more evolved mafic units of the mafic-ultramafic intrusion and Vuurdood Subsuite.*

Downloaded from http://pubs.geoscienceworld.org/gssa/sajg/article-pdf/127/1/55/6373101/55_0011_jogee_et_al.pdf
by University of the Witwatersrand user

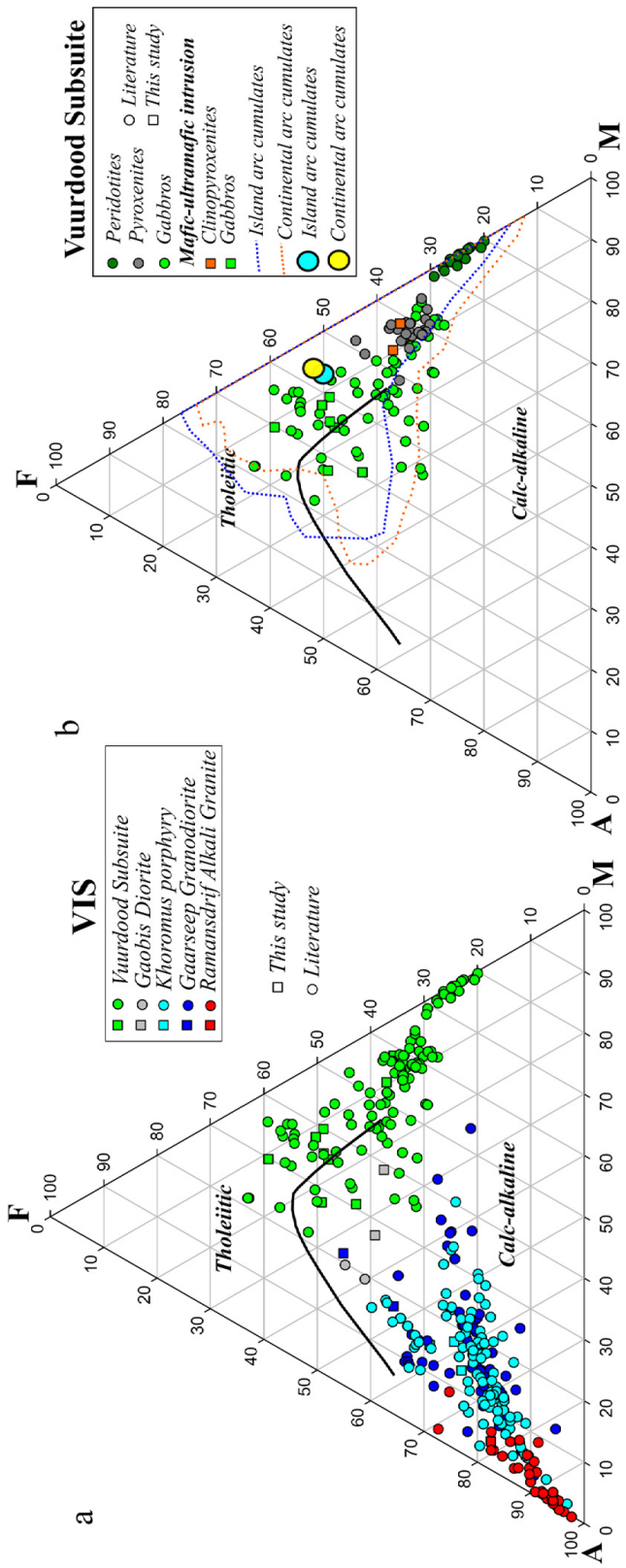


Figure 8. *AFM diagram illustrating the various lithologies of the Vioolsdrif Intrusive Suite (VIS). Felsic units of the Richtersveld Magmatic Arc (RMA) plots in the calc-alkaline trend, whereas the mafic units of the RMA plots in the tholeiitic trend of the diagram. The quartz-feldspar granodiorites of the Khoromus porphyry of the VIS are the host rocks of the Haib deposit. The AFM diagram illustrates that the peridotites and pyroxenites (literature data) as well as clinopyroxenites (this study) plot along the tholeiitic trend, whereas the gabbros (both from literature and in this study) traverse the calc-alkaline and tholeiitic trends. The Vuurdood Subsuite and mafic-ultramafic intrusion plot in the same field as continental and island arc cumulates (Chin et al., 2018).*

Downloaded from http://pubs.geoscienceworld.org/gssa/sajg/article-pdf/127/1/55/6373101/55_0011_jogee_et_al.pdf
by University of the Witwatersrand user

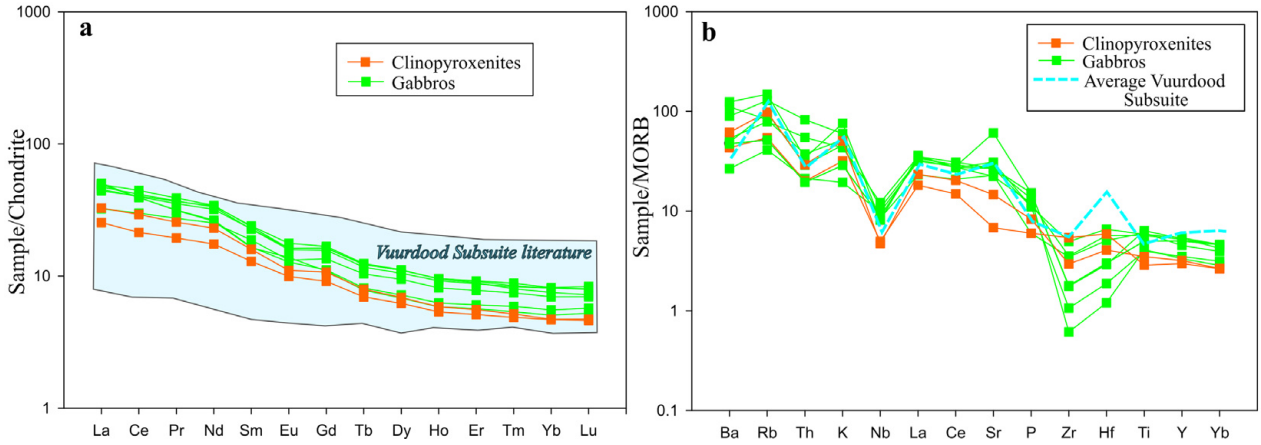


Figure 9. *(**a**) Chondrite-normalised (Anders and Grevesse, 1988) REE patterns for the various rock types of the mafic-ultramafic intrusion: clinopyroxenites have relatively flat patterns, whereas the gabbros show LREE enrichment and minor Eu anomalies, both rock types have very similar patterns, Eu anomalies are identical within uncertainties. (**b**) Mid ocean ridge basalt (MORB)-normalised (White, 2005) multi-element patterns for the various rock types constituting the mafic-ultramafic intrusion and the average Vuurdood Subsuite. The MORB-normalised multi-element patterns for the mafic-ultramafic intrusion and average Vuurdood Subsuite overlap.*

between the clinopyroxenite and gabbro of the mafic-ultramafic intrusion, including: A systematic increase in LILE, and a decrease in Ti. The average MORB-normalised multi-element variation patterns for the mafic-ultramafic intrusion overlap with the Vuurdood Subsuite (Figure 9b).

Machine learning geothermobarometry

A novel machine learning geothermobarometric method was applied in this work to estimate pressure and temperature of crystallisation/equilibration. A detailed explanation of this method is described in Supplementary Information File 6, but broadly involves a machine learning algorithm used to estimate pressure and temperature of clinopyroxene and amphibole crystallisation (Jorgenson et al., 2022; Higgins et al., 2022). This approach, when conducted on geochemical data from pyroxenes and amphiboles from the Vuurdood Subsuite pyroxenites, yield average pressure and temperature estimates of ~4 kbar and 870°C respectively with pressure and temperature ranges from ~1.5 to 7 kbar and ~800 to 900°C (Figure 10). Table 1 shows the average P-T estimates for the Vuurdood Subsuite and the Arizona arclogites (sub-arc residual eclogite facies assemblages dominated by clinopyroxene-garnet-amphibole and iron-titanium oxides) and Tongling cumulates from literature for comparison. The Arizona arclogites represent lower crustal material from a Phanerozoic arc and the Tongling cumulates represents rare cumulate material associated with a Phanerozoic porphyry deposit (Chang and Audetat, 2018; Chen et al., 2020).

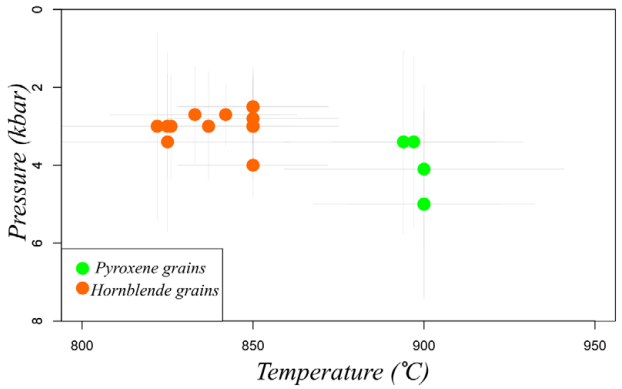


Figure 10. *P-T graph showing the results from the machine learning geothermobarometry conducted on pyroxenes and hornblende grains from the Vuurdood Subsuite pyroxenites. Pressure and temperature, when including procedural uncertainty, ranges, from ~1.5 to 7 kbar and ~800 to 900°C, respectively.*

Table 1. Average pressure and temperature estimates for the Vuurdood Subsuite pyroxenites, Arizona arclogites and Tongling cumulates.

Cumulates	Pressure	Temperature
Vuurdood Subsuite pyroxenites	4 kbar	870°C
Arizona arclogites	25 kbar	725°C
Tongling cumulates	4.7 kbar	980°C

Geochronology of the Kokerboom Intrusion (KI), diorite, and granodiorite

Zircons (~70 to 100 µm in size) separated from gabbro, clinopyroxenite, diorite and granodiorite are euhedral to subhedral, generally stubby to elongate in morphology, show no distinct core and rim domains based on CL imaging and contain inclusions of apatite. Thirty-eight U-Pb isotopic analyses on zircons from the gabbro sample (AJ-21-04) provide a concordia age of 1 878 ± 3 Ma (MSWD = 0.44) (Figure 11a). Thirty-two analyses on zircons from another gabbro sample (AJ-21-23) yielded a concordia age of 1 883 ± 6 Ma (MSWD = 0.71) (Figure 11b). Thirty-five analyses on zircons from the

Downloaded from http://pubs.geoscienceworld.org/gssa/sajg/article-pdf/127/1/55/6373101/55_0011_jogee_et_al.pdf
by University of the Witwatersrand user

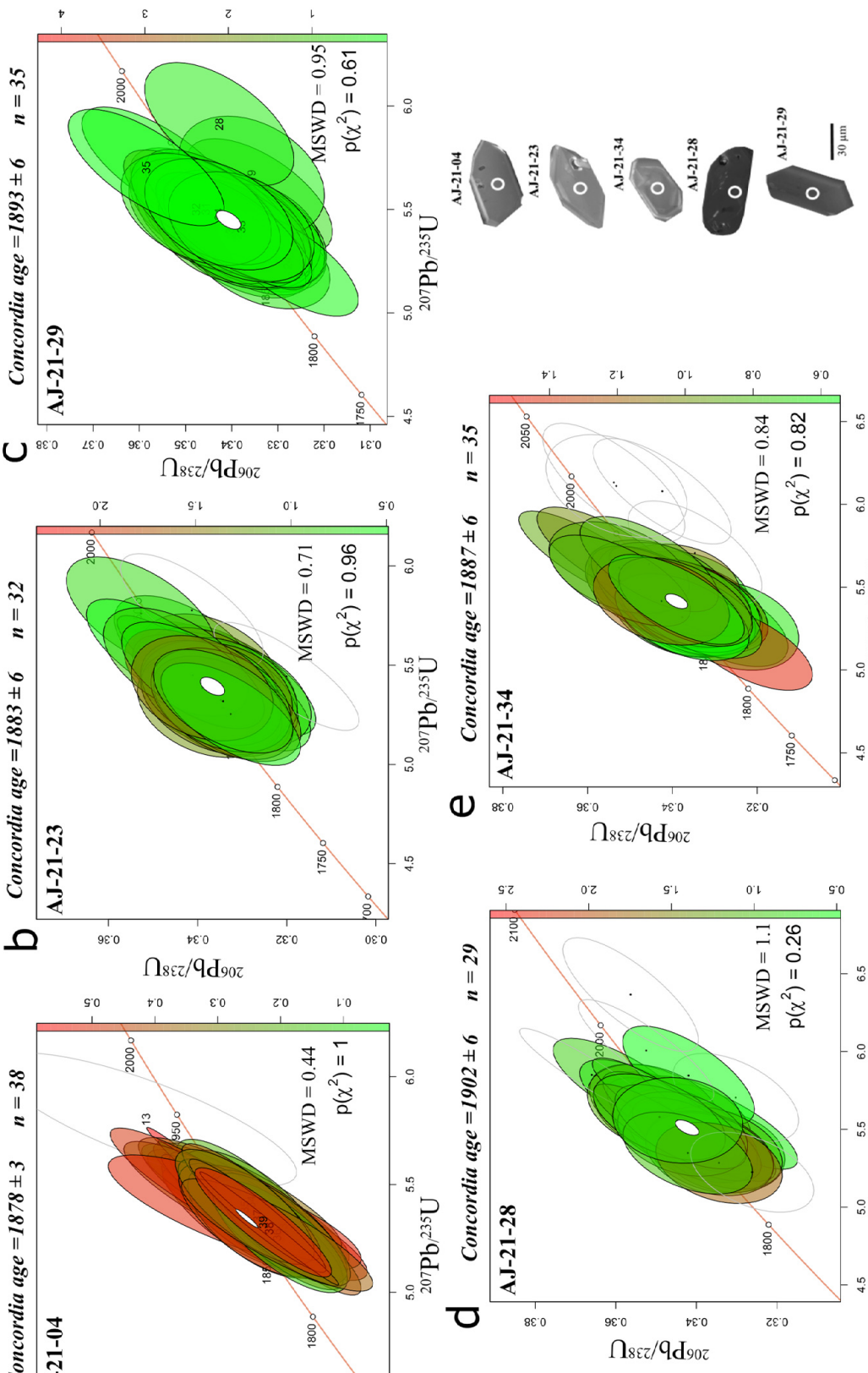


Figure 11. *Wetherill Concordia diagrams illustrating the results from the U-Pb geochronological analyses. The red colours on the diagram indicate discordance and the green colours indicate concordance. Uncertainties on individual isotope ratios are 2 SE (standard error, absolute). The circles indicate laser ablation spots.* ***(a)*** *38 analyses on zircons from the gabbro sample (AJ-21-04) provide a concordia age of 1 878 ± 3 Ma.* ***(b)*** *32 analyses on zircons from the additional gabbro sample (AJ-21-23) yielded a concordia age of 1 883 ± 6 Ma.* ***(c)*** *35 analyses on zircons from the clinopyroxenite sample (AJ-21-29) yielded a concordia age of 1 893 ± 6 Ma.* ***(d)*** *29 analyses on zircons from the granodiorite in contact with the gabbroic intrusion (AJ-21-28) provided a concordia age of 1 902 ± 6 Ma.* ***(e)*** *35 analyses conducted on the diorite sample (AJ-21-34) yielded a concordia age of 1 887 ± 6 Ma. A full compilation of CL and BSE images can be found in the Supplementary Information 5.*

Downloaded from http://pubs.geoscienceworld.org/gssa/sajg/article-pdf/127/1/55/6373101/55_0011_jogee_et_al.pdf
by University of the Witwatersrand user

clinopyroxenite sample (AJ-21-29) yield a concordia age of 1 893 ± 6 Ma (MSWD = 0.95) (Figure 11c). The analyses on the 29 zircons from the granodiorite in contact with the gabbroic intrusion (AJ-21-28) provide a concordia age of 1 902 ± 6 Ma (MSWD = 1.1) (Figure 11d). Thirty-five analyses conducted on the diorite sample (AJ-21-34) yield a concordia age of 1 887 ± 6 Ma (MSWD = 0.84) (Figure 11e). A full compilation of CL and BSE images can be found in the Supplementary Information. The cathodoluminescence images in Figure 11 show representative zircon grains from the samples. The spots shown are the areas that were lasered during the analyses. The red colours on the diagram indicate discordance and the green colours indicate concordance.

Discussion

Previous work has shown that there is a distinct petrological and geochemical link between the ORG, VIS and Vuurdood Subsuite (Reid, 1977; Minnitt, 1979; Macey et al., 2017). Reid (1977), Minnitt (1979) and Macey et al. (2017) stated that the ORG and VIS are comagmatic based on field relationships and geochemical analyses. Reid (1997) proposed that the Vuurdood Subsuite either represents primitive cumulate material of the VIS or could have a different petrogenetic evolution relative to the other units of the VIS. Studies conducted by Reid (1977), Minnaar (2011) and Reid and Minnaar (2021) focused on the Vuurdood Subsuite in the Vioolsdrif area of South Africa. This study focuses on the poorly described mafic-ultramafic intrusion which occurs in the Haib region, Namibia. The mafic-ultramafic intrusion is compared to the Vuurdood Subsuite using combined evidence from geochronology, petrology and geochemistry perspective. Thereafter, we present evidence illustrating that the Haib deposit and the associated mafic-ultramafic intrusion represent the deeper parts of a porphyry system in a convergent margin environment.

The mafic-ultramafic intrusion in the Haib area and the Vuurdood Subsuite

This study reports the first U-Pb zircon ages from the mafic-ultramafic intrusion in Namibia and represent the most recent age determinations on the RMA. The U-Pb ages for the gabbro samples within the mafic-ultramafic intrusion are 1 878 ± 3 Ma and 1 883 ± 6 Ma (Figure 12), while the age for the clinopyroxenite sample is 1 893 ± 6 Ma. A granodiorite in contact with the main gabbroic intrusion returns an age of 1 902 ± 6 Ma. The age data overlap within uncertainty. This granodiorite has been previously mapped as part of the central granodiorite of the Haib area. Age data of the northern granodiorite constrain crystallisation to 1 887 ± 7 Ma (Meng et al., 2021) suggesting that there is more than one intrusive phase of the granodiorites in the Haib region. Given the various ages for the mafic-ultramafic rocks and the granodiorites, it is probable that there were multiple phases of intrusions for the VIS, indicating coeval emplacement of intrusive phases. Macey et al. (2017) also suggested a cyclic model with multiple pulses of mafic to felsic volcanism and plutonism. Age data agree with this cyclic model of multiple pulses rather than a single differentiation event of the Vuurdood Subsuite, to the Goodhouse Subsuite and Ramansdrif Alkali Granite. These new ages for the mafic-ultramafic intrusion in the Haib area overlap with previous age data for the VIS (Supplementary Information 1; Reid, 1987; Grumbley, 2015; Macey et al., 2017; eng et al., 2021) and support the notion that both of these units are coeval members of the VIS. These LA-ICPMS ages also overlap with recent thermal ionisation mass spectrometry (TIMS) zircon ages for the intermediate to felsic rocks of the Haib porphyry deposit reported by Meng et al. (2021), which range between 1920 and 1 880 Ma with a 2σ uncertainty. Furthermore, our ages from the mafic-ultramafic intrusion, agree with unpublished ages from outcrops of the Vuurdood Subsuite in South Africa (unpublished, but reported in Reid and Minnaar, 2021).

In comparison to the mafic-ultramafic intrusions of the Vuurdood Subsuite in the northern Cape, the mafic-ultramafic intrusion near Haib is predominantly composed of the clinopyroxenite and gabbro members, but lacks the peridotitic end member. The alteration assemblages of hornblende-actinolite-chlorite-epidote pseudomorphs after clinopyroxene observed in the mafic-ultramafic intrusion are similar to those observed in the mafic-ultramafic intrusion of the Vuurdood Subsuite. The mafic-ultramafic intrusion shows typical, coarse-grained cumulate textures and is defined by non-cotectic proportions of mineral phases.

As typical cumulates, the major element geochemistry of the mafic-ultramafic intrusion is controlled by the proportion of accumulating phases. This is clearly seen in Figure 7, where the covariation of $Mg^{\#}$ with Al_2O_3, CaO, TiO_2, Na_2O and K_2O is indicative of fractional crystallisation of plagioclase, Fe-Ti oxides, pyroxene and hornblende. Similar trends have been noted in the differentiation sequence of the Vuurdood Subsuite in South Africa, suggesting that the mafic-ultramafic intrusion in the Haib area and the Vuurdood Subsuite form part of the same differentiated suite (Reid, 1987; Miller, 2008 and Macey et al., 2017).

The comagmatic nature of these magmatic units is also corroborated through analysis of typical AFM diagrams (Figure 8), where broad overlap between the Vuurdood Subsuite and the mafic-ultramafic intrusion is observed. The average compositions of mafic cumulates sampled from the Vuurdood Subsuite and the mafic-ultramafic intrusion correspond closely with the average composition of deep- to mid-crustal island and continental arc cumulates (Chin et al., 2018). Together, these mafic and ultramafic cumulates form the earliest stages of a differentiation sequence resembling a calc-alkaline trend with the more felsic volcanic and plutonic members of the VIS.

The REE patterns of the mafic-ultramafic intrusion overlap with patterns of the Vuurdood Subsuite from literature (Figure 9a). These relatively flat REE patterns, lacking significant Eu anomalies, are intriguing given the cumulate nature of this subsuite. Inverse trace element modelling and radiogenic isotope studies are required to fully understand the relationship between these mafic-ultramafic intrusions, the VIS and putative parental, which is beyond the scope of this work. An important interpretation based on the mantle-normalised multi-element variation patterns is the overlap of the mafic-ultramafic intrusion

Downloaded from http://pubs.geoscienceworld.org/gssa/sajg/article-pdf/127/1/55/6373101/55_0011_jogee_et_al.pdf
by University of the Witwatersrand user

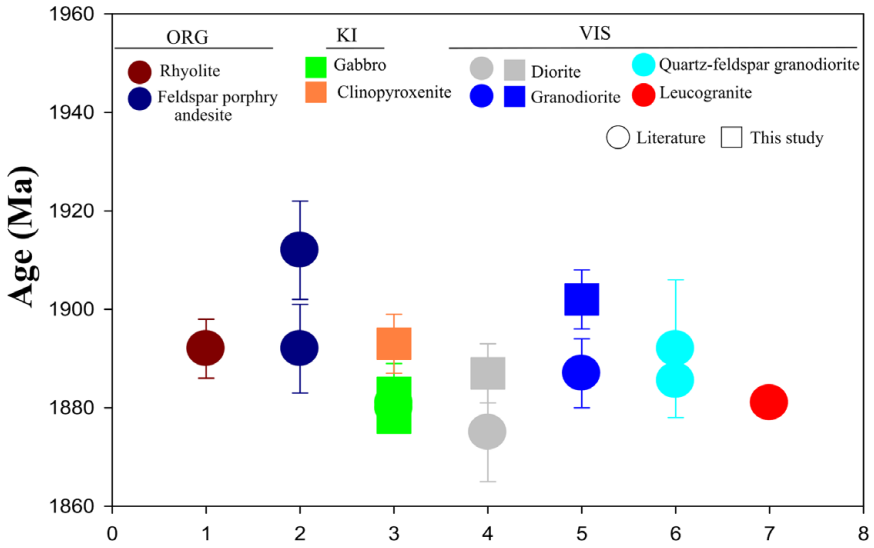


Figure 12. *Compilation of ages for the Orange River Group (ORG), Kokerboom Intrusion (KI) and Vioolsdrif Intrusive Suite (VIS). The data for the ORG and VIS are taken from Meng et al. (2020).*

with the average Vuurdood Subsuite. Together with our new U-Pb age data and machine learning geothermobarometry, we show not only that the mafic-ultramafic intrusion is a coeval and comagmatic component of the Vuurdood Subsuite, but that these magmatic entities represent mid- to upper- crustal cumulates (~12 km depth) formed during construction of the calc-alkaline RMA. As a result of the cogenetic relationship between the poorly described mafic-ultramafic intrusion in the Haib area and the Vuurdood Subsuite, and following the practice of naming discrete ultramafic intrusions of the Vuurdood Subsuite, the mafic-ultramafic intrusion in the Haib area is named the KI in this study.

Evidence for deeper levels of the porphyry system

The KI is intimately associated with the petrogenesis of the Haib porphyry deposit, not only because of their grouping within the VIS, but because the temporal and geochemical relationship (Figure 8). The KI is also in close vicinity (approximately 5 km) of the Haib porphyry deposit.

Several lines of evidence indicate that the Haib deposit and the associated KI preserve the deeper levels of a porphyry system:

- The presence of early dark micaceous veins (the first phase of veins observed in the Haib quartz-feldspar porphyry granodiorites) composed of quartz and coarse mica (Runyon et al., 2017, 2019). Early dark micaceous veins are located at deep levels (palaeodepths of ~4 to 12 km), which is indicative of the root zones of porphyry systems (Runyon et al., 2017 and Runyon et al., 2019).
- Lack of evidence of shallow alteration assemblages, such as propylitic and argillic types (Minnitt, 1979; Minnitt, 1986; Meng et al., 2021).
- Coarse-grained nature of the VIS (clinopyroxenites, granodiorites, diorites, gabbros), indicative of slow cooling at mid-crustal batholith depths (Vermond, 2019).
- The presence of geochemically primitive mafic units such as the gabbros, and clinopyroxenites. The clinopyroxenites are mafic, dense, and usually occur at mid to lower crustal levels (Minnaar, 2012).
- Mineralisation linked with shear fractures, which is indicative of deformation within the ductile regime (5 to 15 km depth) (Davis et al., 2012).
- Finally, geothermobarometry on clinopyroxenes in clinopyroxenites from the Vuurdood Subsuite yield average pressure and temperature estimates of 5 to 15 km depth and 870°C, respectively.

Despite evidence for the Haib being located at deeper levels of the porphyry system, hypabyssal volcanics are present in the Haib area. These volcanics in the vicinity of the Haib porphyry copper deposit have an approximate thickness of 5 to 8 km (Minnitt, 1979), which has previously been cited as the intrusion depth of the Haib porphyries of the Vioolsdrif Suite. Our new geothermobarometry suggests that the emplacement depth of the Vuurdood Subsuite may extend to up 15 km. The mafic-ultramafic cumulates studied here may represent the deeper components of this system.

These lines of evidence agree with and refine previously estimated emplacement pressures of 2 to 3 kbar for the VIS (Minnitt, 1979 and Meng et al., 2021), which according to Minnitt (1979) and Meng et al. (2021) are comparable to deeper sections of Phanerozoic porphyry deposits (such as San-Manuel-Kalamazoo Ore body, Arizona (Lowell and Guilbert, 1970); Fortuna pluton, Chile (Sillitoe, 1973); Los Loros, Chile, Appalachian porphyry systems (Hollister et al., 1974); Cornelia Pluton, Arizona (Wadsworth, 1968), Little Mine Area, Arizona (Durning and Davis, 1978), Laramide porphyry system, Arizona (Seerdoff et al, 2008; Runyon et al., 2017) and Yerington batholith, Nevada (Seerdoff et al, 2008; Runyon et al., 2017). Our refined average pressures of 4 kbar for the mafic-ultramafic

Downloaded from http://pubs.geoscienceworld.org/gssa/sajg/article-pdf/127/1/55/6373101/55_0011_jogee_et_al.pdf
by University of the Witwatersrand user

cumulates of the Vuurdood Subsuite correspond to a crustal depth of ~12 km. These pressures and depths are comparable to the crustal depths of other cumulates formed in porphyry systems and arc environments, such as the Tongling cumulates (~14 km). However, the pressures and temperatures are not comparable with the Arizonan arclogites (20 to 70 km crustal depth) as these occur at much deeper crustal depths. The Tongling cumulates represent rare mid-crustal cumulate material associated with a Phanerozoic porphyry copper deposit (Du and Audetat; 2020), while the Arizonan arclogites represent lower crustal cumulate material (Lee and Tang, 2020).

The KI and the Haib porphyry deposit therefore provide a unique insight into the development of the mid-crustal root zones of a Palaeoproterozoic porphyry deposit.

Conclusion

The purpose of this work was to establish a possible link between the mafic-ultramafic intrusion in the Haib area and the Vuurdood Subsuite. Petrological, geochemical and geochronological observations document that the KI (the name given to the mafic-ultramafic intrusion in this study) is a continuation of the Vuurdood Subsuite into Namibia, but is crucially associated with Cu mineralisation of the Haib. These similarities include lithological variation within the intrusion, mineral and alteration assemblages, major and trace element geochemistry and U-Pb zircon age data. The overlap of the major element compositions shown by the AFM diagram for the KI and Vuurdood Subsuite with the lower crustal cumulates in both island and continental arc settings is significant and provides evidence in favour of an arc tectonic setting for these Richtersveld lithologies based on the cumulate nature. The sulphides in the clinopyroxenite are significant and confirm studies by Wilkinson (2013), Du and Audetat (2020) and Chen et al. (2020), which proposed that early sulphide saturation is not detrimental to porphyry copper metallogenesis. Magmatic sulphides are observed in the lower arc sections of the Talkeetna gabbros, Khohistan cumulates, Arizona garnet pyroxenite cumulates, as well as in the amphibole-rich cumulate xenoliths and amphibole megacrysts of the Late Jurassic to Early Cretaceous (~147 to 136 Ma) Tongling porphyry deposit (Deng et al., 2007; Wu et al., 2010; Audetat and Simon, 2012; Lee et al., 2012; Hou et al., 2017; Jenner, 2017; Chang and Audetat, 2018; Chen et al., 2020). The amphibole-rich cumulate xenoliths and amphibole megacrysts of the Late Jurassic to Early Cretaceous Tongling deposit are linked to porphyry copper formation. Based on observations from Phanerozoic porphyry copper deposits that are related with cumulate material at mid- to lower crustal levels, such as the Tongling deposit, the KI may either represent a cumulate source for the Haib deposit magmas or could simply be the cumulate counterpart to the magmas forming this porphyry intrusion. These notions need to be tested using other geochemical approaches, e.g. inverse trace element modelling and radiogenic isotope analyses. A link between the KI and the Haib porphyry copper deposit can also be established based on the overlapping ages of the KI and the Haib mineralisation. Future work may aim at conducting copper and iron isotope analyses on the Haib deposit, which will shed light on our global understanding of the metallogenesis of porphyry copper deposits from both a temporal and trans-crustal perspective, as the Haib deposit is Palaeoproterozoic in age when compared to predominantly Phanerozoic porphyry deposits. The Haib deposit represents deeper levels of the porphyry system in contrast to shallower level younger Phanerozoic porphyry deposits.

Acknowledgements

This research was funded by the National Research Foundation. We would like to extend our gratitude to Deep-South Resources for the field access and assistance. To Caiphas Majola, Sam Tshabalala and Louis Mudalahothe, thank you for the logistical and sample preparation assistance. To Marlin Patchappa, Nonkuselo Madlakana and Ryan Mathur, your assistance with analytical lab work and raw data processing is much appreciated. Robert Bolhar acknowledges financial support to establish the LA-SF-ICPMS facility at the University of Witwatersrand through a NRF-NEP grant (UID 105674). Gratitude is also extended to Bob Thomas and an anonymous reviewer, as well as editor Marlina Elburg, for their constructive comments which significantly improved this manuscript.

References

Audétat, A. and Simon, A.C., 2012. Magmatic controls on porphyry copper genesis. In: J.W. Hedenquist, M. Harris and F. Camus (Editors), Geology and genesis of major copper deposits and districts of the world: a tribute to Richard H Sillitoe. Society of Economic Geologists, 16, 553-572.

Barr, J.M. and Reid, D.L., 1992. Hydrothermal alteration at the Haib porphyry copper deposit, Namibia: Stable isotope and fluid inclusion patterns. Communications of the Geological Survey of Namibia, 8, 23-35.

Bilenker, L.D., Simon, A.C., Reich, M., Lundstrom, C.C., Gajos, N., Bindeman, I., Barra, F. and Munizaga, R., 2016. Fe-O stable isotope pairs elucidate a high-temperature origin of Chilean iron oxide-apatite deposits. Geochimica et Cosmochimica Acta, 177, 94-104.

Chang, J. and Audétat, A., 2018. Petrogenesis and metal content of hornblende-rich xenoliths from two Laramide-age magma systems in southwestern USA: Insights into the metal budget of arc magmas. Journal of Petrology, 59, 1869-1898.

Chelle-Michou, C., Rottier, B., Caricchi, L. and Simpson, G., 2017. Tempo of magma degassing and the genesis of porphyry copper deposits. Science Reports, 7, 40566.

Chen, K., Tang, M., Lee, C.T.A., Wang, Z., Zou, Z., Hu Z. and Liu, Y., 2020. Sulfide-bearing cumulates in deep continental arcs: The missing copper reservoir. Earth and Planetary Science Letters, 531, 115971.

Childress, T. M., Simon, A. C., Day, W. C., Lundstrom, C. C. and Bindeman, I. N., 2016. Iron and oxygen isotope signatures of the Pea Ridge and Pilot Knob magnetite-apatite deposits, southeast Missouri, USA. Economic Geology, 111, 2033-2044.

Chin, E.J., Shimizu, K., Bybee, G.M. and Erdman, M.E., 2018. On the development of the calc-alkaline and tholeiitic magma series: a deep crustal cumulate perspective. Earth and Planetary Science Letters, 482, 277-287.

Cline, J.S. and Bodnar, R.J., 1991. Can economic porphyry copper mineralisation be generated by a typical calc-alkaline melt. Journal for Geophysical Research Solid Earth, 96, 8113-8126.

Colliston, W.P. and Schoch, A.E., 2000. Mid-Proterozoic tectonic evolution along the Orange River on the border between South Africa and Namibia. Communications of the Geological Survey of Namibia, 12, 57-66.

Cornell, D.H., Thomas, R.J., Moen, H.F.G., Reid, D.L., Moore, J.M. and Gibson, R.L., 2006. The Namaqua-natal province. In: M.R. Johnson, C.R. Anhaeusser and R.J. Thomas (Editors), The Geology of South Africa. Geological Society of

Downloaded from http://pubs.geoscienceworld.org/gssa/sajg/article-pdf/127/1/55/6373101/55_0011_jogee_et_al.pdf
by University of the Witwatersrand user

South Africa and Council for Geoscience, South Africa, 325-379.

Davis, G.H., Reynolds, S.J. and Kluth, C.F., 2012. Structural Geology of Rocks and Regions. Wiley, 3rd edition.

Du, J. and Audétat, A., 2020. Early sulfide saturation is not detrimental to porphyry Cu-Au formation. Geology, 48, 519-524.

Duan, J., Tang, J., Li, Y., Liu, S.A., Wang, Q., Yang, C. and Wang, Y., 2015. Copper isotopic signature of the Tiegelongnan high-sulfidation copper deposit, Tibet: implications for its origin and mineral exploration. Mineralium Deposita, 51, 591-602.

Ducea, M.N., Bowman, E., Chapman, A.D. and Balica, C., 2020. Arclogites and their role in continental evolution; Part 1: Background, locations, petrography, geochemistry, chronology and thermobarometry. Earth-Science Reviews, 214, 1-16.

Durning, W.P. and Davids, J.D., 1978. The root-zone characteristics of porphyry copper deposits. Arizona Geological Digest, 11, 81-89.

Gagnevin, D., Boyce, A., Barrie, C., Menuge, J. and Blakeman, R., 2012. Zn, Fe and S isotope fractionation in a large hydrothermal system. Geochimica et Cosmochimica Acta, 88, 183-198.

Gao, Z., Zhu, X., Sun, J., Luo Z., Bao, C., Tang, C. and Ma, J., 2018. Spatial evolution of Zn-Fe-Pb isotopes of sphalerite within a single ore body: a case study from the Dongshengmiao ore deposit, Inner Mongolia, China. Mineralium Deposita., 53, 55-65.

Gregory, M.J. and Mathur, R., 2017. Understanding copper isotope behavior in the high temperature magmatic-hydrothermal porphyry environment. Geochemistry, Geophysics, Geosystems, 18, 4000-4015.

Grumbley, N.L., 2015. The Geological Evolution of the Haib Cu-Mo Porphyry, Namibia. MSc thesis (unpublished), Trinity College Dublin, 175pp

Hannah, J., Stein, H., Wieser, M., De Laeter, J. and Varner, M., 2007. Molybdenum isotope variations in molybdenite: vapor transport and Rayleigh fractionation of Mo. Geology, 35, 703-706.

Hao, H., Campbell, I.H., Park, J.-W. and Cooke, D.R., 2017. Platinum-group element geochemistry used to determine Cu and Au fertility in the Northparkes igneous suites, New South Wales, Geochimica et Cosmochimica Acta, Australia. 216, 372-392.

He, Z.W., Zhang, X.C., Deng, X.D., Hu, H., Li, Y., Yu, H., Archer, C., Li, J.W. and Huang, F., 2020. The behavior of Fe and S isotopes in porphyry copper systems: constraints from the Tongshankou Cu-Mo deposit, Eastern China. Geochimica et Cosmochimica Acta., 270, 61-83.

Hollister, V.F., Potter, R.R. and Barker, A.C., 1974. Porphyry-type deposits of the Appalachian orogen. Economic Geology, 69, 618-630.

Holwell, D.A., Fiorentini, M.L., Knott, T.R., McDonald, I., Blanks, D.E., McCuaig, T.C. and Gorczyk, W., 2022. Mobilisation of deep crustal sulfide melts as a first order control on upper lithospheric metallogeny. Nature Communications, 13, 573.

Jenner, F.E., 2017. Cumulate causes for the low contents of sulfide-loving elements in the continental crust. Nature Geoscience, 10, 524-529.

Jenner, F.E., O'Neill, H.C., Arculus, R.J. and Mavrogenes, J.A., 2010. The magnetite crisis in the evolution of arc-related magmas and the initial concentrations of Au, Ag and Cu. Journal of Petrology, 51, 2445-2464.

Jorgenson, C., Higgins, O., Petrelli, M., Bégué, F. and Caricchi, L., 2022. A Machine Learning based approach to clinopyroxene thermobarometry model optimization and distribution for use in earth sciences. Journal of Geophysical Research: Solid Earth, 127, 1-21

Joubert, P., 1986. Namaqualand – A model of Proterozoic accretion? Transactions of the Geological Society of South Africa, 89, 79-96.

Knipping, J.L., Bilenker, L.D., Simon, A.C., Reich, M., Barra, F., Deditius, A.P., Lundstrom, C., Bindeman, I. and Munizaga, R., 2015. Giant Kiruna-type deposits form by efficient flotation of magmatic magnetite suspensions. Geology, 43, 591-594.

Lee, C.-T.A. and Tang, M., 2020. How to makes porphyry copper deposit. Earth and Planetary Science Letters, 529, 1-11.

Lee, C-T.A. and Anderson, D., 2015. Continental crust formation at arcs, the arclogite "delamination" cycle, and one origin for fertile melting anomalies in the mantle. Science Bulletin, 60, 1141-1156.

Lee, C-T.A., Luffi, P., Chin, E.J., Bouchet, R., Dasgupta, R., Morton, D.M., Le Roux, V., Xin, Q.-z. and Jin, D., 2012. Copper systematics in arc magmas and implications for crust-mantle differentiation. Science, 336, 64-68.

Li, W.Q., Jackson, S.E., Pearson, N.J. and Graham, S., 2010a. Copper isotopic zonation in the Northparkes porphyry Cu-Au deposit, SE Australia. Geochimica et Cosmochimica Acta, 74, 4078-4096.

Lowell, J.D. and Guilbert, J.M., 1970. Lateral and vertical alteration-mineralisation zoning in porphyry ore deposits. Economic Geology, 65, 373-408.

Macey, P.H., Thomas, R.J., Minnaar, H.M., Gresse, P.G., Lambert, C.W., Groenewald, C.A., Miller, J.A., Indongo, J.I., Angombe, M., Shifotoka, G., Frei, D., Diener, J.F.A., Kisters, A.F.M., Dhansay, T., Smith, H., Doggart, S., le Roux, P., Hartnady, M.I. and Tinguely, C., 2017. Origin and evolution of the 1.9 Ga Richtersveld Magmatic Arc, SW Africa. Precambrian Research, 292, 417-451.

Markl, G., Lahaye, Y. and Schwinn, G., 2006. Copper isotopes as monitors of redox processes in hydrothermal mineralisation. Geochimica et Cosmochimica Acta., 70, 4215-4228.

Mathur, R., Jin, L., Prush, V., Paul, J., Ebersole, C., Fornadel, A., Williams, J.Z. and Brantley, S., 2012. Cu isotopes and concentrations during weathering of black shale of the Marcellus Formation, Huntingdon County, Pennsylvania (USA). Chemical Geology, 304-305, 175-184.

Meng et al., 2021. Oxidized sulfur-rich arc magmas formed porphyry Cu deposits by 1.88 Ga. Nature Communications, 12, 2189.

Miller, R., McG., 2008. The geology of Namibia. Handbook, Geological Survey of Namibia, 3, 5-15.

Minnaar, H., 2012. Composition and evolution of the Proterozoic Vioolsdrif Batholith (including the Orange River Group), northern Cape Province, South Africa. Ph.D. thesis (unpublished). University of the Free State, 209pp

Minnitt, R.C.A., 1979. The geological setting of porphyry-type copper mineralisation in the Haib River area, South West Africa. Ph.D. thesis (unpublished), University of the Witwatersrand, Johannesburg, 366pp

Minnitt, R.C.A., 1986. Porphyry Copper-Molybdenum Mineralisation at Haib River, South West Africa/Namibia. Mineral Deposits of Southern Africa, In: C.R. Anhaeusser and S. Maske (Editors), Mineral Deposits of Southern Africa, v. II: The Geological Society of South Africa, 1567-1585.

Müller, D., Franz, L., Herzig, P.M. and Steve, H., 2001. Potassic igneous rocks from the vicinity of epithermal gold mineralisation, Lihir Island, Papua New Guinea. Lithos, 57, 163-186.

Norrish, K. and Hutton, J.T., 1969. An accurate X-ray spectrographic method for the analysis of geologic samples. Geochemica et Cosmochimica Acta, 33, 431-454.

Park, J.-W., Campbell, I.H., Kim, J. and Moon, J.-W., 2015. The role of late sulfide saturation in the formation of a Cu- and Au-rich magma: Insights from the platinum-group geochemistry of Niuatahi-Motutahi lavas, Tonga rear arc. Journal of Petrology, 56, 59-81.

Park, J.-W., Campbell, I.H., Malaviarachchi, S.P.K., Cocker, H., Hao, H. and Kay, S.M., 2019. Chalcophile element fertility and the formation of porphyry Cu ± Au deposits. Mineralium Deposita, 54, 657-670.

Petrus, J.A. and Kamber, B.S., 2012. VizualAge: A novel approach to laser ablation ICP-MS U-Pb geochronology data reduction. Geostandards and Geoanalytical Research, 36, 247-270.

Reid, D. L., Welke, H. J., Erlank, A. J. and Moyes, A. B., 1987. The Orange River Group, a Proterozoic volcanic belt in the western Namaqua Province, South Africa. Geochemistry and mineralisation of Proterozoic volcanic suites. In: T.C. Pharaoh, R.D. Beckinsale and D.T. Rickard (Editors), Special Publication Geological Society 33, 327-346.

Reid, D.L., 1977. The geochemistry of Precambrian igneous rocks in the lower Orange River region., Ph.D. thesis (unpublished), University of Cape Town, South Africa, 396pp

Reid, D.L., 1979. Petrogenesis of calc-alkaline metalavas in the mid-Proterozoic Haib Volcanic Subgroup, lower Orange River region. Transactions of the Geological Society of South Africa, 82, 109-131.

Reid, D.L., 1979a. Age relationships within the mid-Proterozoic Vioolsdrif Batholith, lower Orange River region. Transactions of the Geological Society of South Africa, 82, 305-311.

Reid, D.L., 1979b. Total rock Rb-Sr and U-Th-Pb isotopic study of Precambrian metavolcanic rocks in the Lower Orange River region. Earth Planetary Science Letters, 42, 368-378.

Reid, D.L., 1997. Sm-Nd age and REE geochemistry of Proterozoic arc-related igneous rocks in the Richtersveld Subprovince, Namaqua Mobile Belt, Southern Africa. Journal of African Earth Sciences, 24, 621-633.

Downloaded from http://pubs.geoscienceworld.org/gssa/sajg/article-pdf/127/1/55/6373101/55_0011_jogee_et_al.pdf
by University of the Witwatersrand user

Reid, D.L. and Minnaar, H., 2021. Lithostratigraphy of the Vuurdood Subsuite, an early mafic-ultramafic phase of the Palaeoproterozoic Vioolsdrif Intrusive Suite, Richtersveld Magmatic Arc, Northern Cape Province. South African Journal of Geology, 124, 805-814.

Runyon, S.E., Seedorff, E., Barton, M.D., Steele-MacInnis, M., Lecumberri-Sanchez, P. and Mazdab F.K., 2019. Coarse muscovite veins and alteration in porphyry systems. Ore Geology Reviews, 113, 1-32.

Runyon, S.E., Steele-MacInnis, M., Seedorff, E., Lecumberri-Sanchez, P. and Mazdab F.K., 2017. Coarse muscovite veins and alteration deep in the Yerington batholith, Nevada: insights into fluid exsolution in the roots of porphyry copper systems. Mineralium Deposita, 52, 463-470.

Seedorff, E., Barton, M.D., Stavast, W.J.A. and Maher, D.J., 2008. Root zones of porphyry systems: extending the porphyry model to depth. Economic Geology, 103, 939-956.

Sillitoe, R. H., 1973. The tops and bottoms of porphyry copper deposits. Economic Geology, 68, 799-815.

van Niekerk H.S., Elburg, M.A., Andersen, T. and Armstrong, R.A., 2022. Provenance of metasedimentary rocks of the Kheis Terrane and Kakamas Domain: support for accretionary tectonics during the development of the western Namaqua-Natal metamorphic province. South African Journal of Geology, 125, 61-78.

Vermeesch, P., 2018. IsoplotR: a free and open toolbox for geochronology. Geoscience Frontiers, 9, 1479-1493.

Vermond, D., 2019. Identifying the controls on mineralisation and re-defining the evolution of the Haib porphyry Cu deposit. M.Sc. thesis (unpublished), Camborne School of Mines, University of Exeter, 76pp

Wadsworth, W.B., 1968. The Cornelia pluton, Ajo, Arizona. Economic Geology, 63, 101-115.

Walker, P.W.A. and Richards, D.S., 2018. Independent Technical Review and Resource Estimate – The Haib Copper Porphyry Project, Namibia, Deep-South Resources Inc.

Wang, Y., Zhu, X.K., Mao, J.W., Li, Z.H. and Cheng, Y.B., 2011. Iron isotope fractionation during skarn-type metallogeny: a case study of Xinqiao Cu-S-Fe-Au deposit in the Middle-Lower Yangtze Valley. Ore Geology Reviews, 43, 194-202.

Wilkinson, J., 2013. Triggers for the formation of porphyry ore deposits in magmatic arcs. Nature Geoscience, 6, 917-925.

Yao, J., Mathur R., Sun, W., Song, W., Chen, H., Mutti, L., Xiang, X. and Luo, X., 2016. Fractionation of Cu and Mo isotopes caused by vapor-liquid partitioning, evidence from the Dahutang W-Cu-Mo ore field. Geochemistry, Geophysics, Geosystems, 17, 1725-1739.

Zhang, D. and Audétat, A., 2017. What caused the formation of the giant Bingham Canyon porphyry Cu-Mo-Au deposit? Insights from melt inclusions and magmatic sulfides. Economic Geology, 112, 221–244.

Editorial handling: M.A. Elburg.

Downloaded from http://pubs.geoscienceworld.org/gssa/sajg/article-pdf/127/1/55/6373101/55_0011_jogee_et_al.pdf
by University of the Witwatersrand user